TISSUE ENGINEERING: Part C
Volume 23, Number 10, 2017
Mary Ann Liebert, Inc.
DOI: 10.1089/ten.tec.2017.0078

termis
Tissue Engineering
& Regenerative Medicine
International Society

METHODS ARTICLE

Collagen and Hydroxyapatite Scaffolds Activate Distinct Osteogenesis Signaling Pathways in Adult Adipose-Derived Multipotent Stromal Cells

Wei Duan, MS, PhD,[1] Masudul Haque, PhD,[1] Michael T. Kearney, MApStat,[2] and Mandi J. Lopez, DVM, MS, PhD[1]

Osteogenic cell signaling pathway disruption varies among bone diseases. This investigation was designed to identify adipose-derived multipotent stromal cell (ASC) and bone graft scaffold combinations for local, targeted restoration of gene expression and extracellular matrix (ECM) deposition. Human ASC osteogenesis on bone graft materials was quantified following culture in stromal (S), osteogenic (O), or osteogenic for 48 h followed by stromal medium (OS) to test the two-part hypothesis: (1) identical ASC isolates on distinct bone graft scaffolds demonstrate unique viability, differentiation, ECM production, and gene expression in the same culture conditions; (2) identical ASC-bone graft scaffold combinations have different cell viability, differentiation, ECM production, and gene expression when cultured in S, O, or OS medium. Three commercially available bone graft scaffold materials, type I bovine collagen (C), hydroxyapatite + β-tricalcium phosphate + type I bovine collagen (HT), and β-tricalcium phosphate + type I bovine collagen (CT) were evaluated. Passage 3 ASCs were loaded onto scaffold blocks with a spinner flask bioreactor, and constructs were cultured up to 28 days. Cell viability, gene expression (alkaline phosphatase [*ALPL*], osteoprotegerin [*TNFRSF11B*], osteocalcin [*BGLAP*], cannabinoid receptors type I [*CNR1*] and II [*CNR2*], receptor activator of nuclear factor kappa β ligand [*TNFSF11*]), as well as ECM DNA, collagen, sulfated glycosaminoglycan, and protein content were quantified. Matrix organization was evaluated with scanning electron microscopy. Effects of scaffold, medium, or culture duration on cell viability were minimal. Significantly higher initial *ALPL* expression decreased with time, while *BGLAP* expression increased in HT constructs in O medium, and the constructs had the most abundant ECM components and ultrastructural organization. There was a similar, although delayed, pattern of gene expression and greater ECM collagen with less organization in C constructs in O medium. Higher *CNR1* expression in C versus higher *TNFRSF11B/TNFSF11* expression in HT constructs throughout the study support stimulation of unique osteogenic signaling pathways by identical cell isolates. These results suggest that bone scaffold composition may be used to selectively target specific osteogenic cell signaling pathways in ASC constructs to stimulate ECM deposition based on therapeutic needs.

Keywords: cannabinoid, bioreactor, bone, graft, stem cell

Introduction

Bone grafts are a standard therapy to augment osteogenesis, but autografts can be complicated by limited graft material and harvest morbidity and allografts by disease transmission and immunogenicity.[1,2] Bone graft substitutes offer plentiful, risk-free options that are not influenced by donor condition.[3] Adipose-derived multipotent stromal cells (ASCs) increase osteoinduction and osteoconduction of commercially available, bone graft substitutes.[1,4] Advantages such as a greater number and volume of tissue harvest depots, in addition to higher stromal cell density and comparable plasticity to bone marrow-derived multipotent stromal cells (BMSCs), make ASCs an appealing choice for MSC–scaffold constructs.[5] However, recipient factors such as age, sex, and health influence the ability of ASCs to promote bone formation.[6,7] Customization of ASC-bone graft constructs for individual morbidities will elevate current standards of care.

[1]Laboratory for Equine and Comparative Orthopedic Research, School of Veterinary Medicine, Louisiana State University, Baton Rouge, Louisiana.
[2]Department of Pathobiological Sciences, Louisiana State University, Baton Rouge, Louisiana.

Osteogenesis is a dynamic, multifaceted process with intersecting cell signaling cascades that direct cell recruitment, differentiation, maturation, and behavior.[8] Bone-forming capacity is reduced by cell signaling pathway modifications from disease or age.[8–10] Osteoblastic and osteoclastic activity is regulated by the ratio of osteoprotegerin (*TNFRSF11B*) and receptor activator of nuclear factor kappa β ligand (*TNFSF11*), and alterations are thought to contribute to abnormal bone healing and maintenance in several bone diseases.[8] Activity levels of cannabinoid receptors type I (*CNR1*) and II (*CNR2*) are implicated in age-related changes in bone turnover and mass.[9–12] Notably, *TNFRSF11B* stimulation triggers Wnt/β catenin signaling, while the cannabinoid receptors appear to work via adrenergic signaling.[8,13,14] This knowledge provides an opportunity to explore targeted restoration of specific osteogenic pathways with ASC-bone graft constructs. Specifically, the ability to confidently restore cell signaling most strongly associated with compromised bone formation of individual patients will contribute to improved and customized treatment options.

Commercially available bone grafts are composed of inorganic and organic components to direct cell differentiation and extracellular matrix (ECM) production.[1,3,15–18] The type and amount of inorganic crystals as well as their ratios to each other and proteins stimulate distinct gene expression.[16,19–24] Cells also behave differently on identical scaffolds when cultured in environments designed to maintain a primordial state versus those to promote differentiation and maturation.[25,26] Mechanisms to ''prime'' cells by short-term exposure to induction reagents may accelerate differentiation stimulated by the scaffold.[27]

We propose that it is possible to reproducibly select for specific ASC osteogenesis signaling pathways with scaffold composition and/or culture medium. To evaluate this potential, *in vitro* human adult ASC viability, gene expression, and ECM deposition and organization was determined on bone graft scaffolds composed of pure type I collagen, type I collagen and one mineral, β tricalcium phosphate, and type I collagen with two minerals, β tricalcium phosphate, and hydroxyapatite (HA). Cell–scaffold combinations were evaluated following culture in stromal (S), osteogenic (O), or short-term osteogenic followed by stromal medium (OS) for up to 28 days. The following two-part hypothesis was tested: (1) Identical ASC isolates on distinct bone graft scaffolds demonstrate unique viability, differentiation, ECM production, and gene expression in the same culture conditions; (2) Identical ASC-bone graft scaffold combinations have unique cell viability, differentiation, ECM production, and gene expression when cultured in S, O, or OS medium. The overarching goal of this investigation was to identify ASC-scaffold combinations for local, targeted restoration of genetic expression and ECM deposition to enhance bone healing in the presence of specific bone pathology.

Materials and Methods

Ethics statement

All the procedures were approved by the Institutional Review Board (Protocol #00006218) and informed consent was obtained before tissue use.

Study design

Commercially available human ASCs (LaCell LLC, New Orleans, LA) were culture expanded to cell passage (P) 3. Cell viability was quantified with confocal laser microscopy immediately after loading and 7 and 14 days of culture. Gene expression (alkaline phosphatase [*ALPL*], collagen 1α1 [*COL1A1*], osteocalcin [*BGLAP*], *CNR1*, *CNR2*, *TNFRSF11B*, and *TNFSF11*, and ECM deposition (double-stranded DNA [dsDNA], total protein, sulfated glycosaminoglycan [sGAG], total collagen) in ASC-scaffold constructs were quantified before and after 7, 14, and 28 days of culture in S, O, and OS medium. Scanning electron microscopy (SEM) was used to assess scaffolds without cells and extracellular matrix on constructs after 7 and 14 days of culture. Specifically, the sample set consisted of ASCs from three donors that were each loaded on three distinct scaffolds and immediately assessed or evaluated after culture in three different media for 7, 14, or 28 days for all measures except cell viability and SEM, which were each performed after the first two. A minimum of three replicates of each assay were performed for all samples.

Scaffold materials

Bone graft scaffolds were composed of type I bovine collagen (C, Avitene™ Ultrafoam™; Davol, Inc., Warwick, RI), 15% HA, 85% β-tricalcium phosphate, type I bovine collagen (HT, MasterGraft™ Matrix; Medtronic Sofamor Danek, Inc., Minneapolis, MN) and 20% type I bovine collagen, and 80% β tricalcium phosphate (CT, Vitoss® Scaffold Foam™; Stryker Corp., Kalamazoo, MI). Scaffolds were aseptically cut into $5\times5\times3$ mm (C), $5\times5\times5$ mm (HT), and $5\times5\times4$ mm (CT) rectangular blocks for constructs.

Cells

Frozen ASC aliquots (LaCell; LLC, New Orleans, LA) from one male and two females (47.3 ± 7.0 years (mean ± standard error of the mean [SEM]), 28.3 ± 4.1 BMI) in cryopreservation medium (LaCryoM-100, LaCell, LLC) were used for this study.[28] Aliquots were thawed at 37°C with agitation for 2–3 min, combined with 5 mL of stromal medium (S, DMEM/F12 [Hyclone, Logan, UT], 10% characterized fetal bovine serum [Hyclone], and 1% antibiotic [MP Biochemicals, Solon, OH]) and centrifuged (300 *g*, 5 min). Cells were culture expanded to P3 in S medium (37°C, 5% CO_2) with an initial seeding density of 5×10^3 cells/cm^2, medium changes every 3 days and passage at ~70% confluence.[29]

Cell loading

Passage 3 ASC suspensions (17.0×10^6 cells/120 mL corresponding to 5.7×10^4 cells/mm^3 of total scaffold volume) from each donor were loaded onto three scaffolds of each composition on 3, 4-inch-long, 22 g spinal needles suspended from a rubber stopper in 100-mL spinner flasks (Bellco® Biotechnology, Newark, NJ). The process was repeated five times for each donor (15 samples/scaffold/donor). Scaffolds were oriented with the shortest dimension perpendicular to the needle long axis. Spinner flasks were maintained in a humidified incubator (37°C, 5% CO_2) for 2 h with a magnetic stir bar rotating at 70 rpm. Following cell loading, loading efficiency was calculated from the number of cells remaining in each flask. Samples were evaluated or transferred to one of three media in six-well culture plates (Thermo Fisher Scientific, Waltham, MA): (1) stromal (S, DMEM/F12 [Hyclone, Logan, UT], 10% characterized fetal bovine serum [Hyclone], and 1%

antibiotic [MP Biochemicals, Solon, OH]); (2) osteogenic (O, stromal +10 mM β-glycerophosphate [Affymetrix, Santa Clara, CA], 20 nM dexamethasone [Sigma-Aldrich, St. Louis, MO], and 0.05 mM ascorbic acid [Sigma-Aldrich]); or (3) osteogenic for 48 h followed by stromal (OS).

Cell viability (days 0, 7, 14)

Cell viability was quantified on 20 digital photomicrographs (TIFF, 10×) of the construct surface, 250 μm apart, that were generated with a spectral confocal laser scanning microscope digital imaging system (Leica TCS SP2; Leica Microsystems, Buffalo Grove, IL). Constructs were rinsed with phosphate-buffered saline and incubated at room temperature in darkness with assay reagents (Invitrogen LIVE/DEAD® Viability/Cytotoxicity kit; Thermo Fisher Scientific) for 30 min.[30] The numbers of live (green) and dead (red) cells in each section were quantified (Image-Pro; Media Cybernetics, Bethesda, MD) to calculate live cell percentage (live cells/total cells × 100) for each construct.

Gene expression (days 7, 14, 28)

Total RNA was extracted from cell–scaffold constructs (RNeasy Plus Mini Kit; Qiagen, Germantown, MD) and cDNA synthesized (QuantiTect Reverse Transcription Kit; Qiagen). Quantification of target gene levels (*ALPL*, *BGLAP*, *CNR1*, *CNR2*, *TNFRSF11B*, and *TNFSF11*) was performed with a 384-well plate sequence detection system (ABI Prism 7900HT; Applied Biosystems, Carlsbad, CA) using SYBR Green Supermix (Bio-Rad Laboratories, Hercules, CA) and validated primer sequences (Table 1). The $2^{-\Delta\Delta Ct}$ values were determined relative to the reference gene glyceraldehyde 3-phosphate dehydrogenase [*GAPDH*] and target gene expression immediately after cell loading (day 0). The *TNFRSF11B/TNFSF11* ratio was determined in individual samples by dividing the *TNFSF11B* fold change by the *TNFSF11* fold change.

Compositional analysis (days 7, 14, 28)

Cell–scaffold constructs were lyophilized (–55°C, 0.2 mbar, 4 h) and then incubated in a papain digest (2 mg papain [MP Biomedicals]/g lyophilized sample, 20 mM L-cysteine [MP Biomedicals], 9 mM disodium EDTA [Sigma-Aldrich], and 3.6 M sodium acetate [Sigma-Aldrich]) at 60°C for 10 h. Following centrifugation of the solution (4000 *g*, 10 min), the supernatant was collected and stored at −80°C. Samples were thawed for 1 min in a 37°C water bath immediately before compositional analysis. All assays were performed according to manufacturer's instructions or published methods for microtiter plate analysis and fluorescence or absorbance quantified with a multiwell plate reader (Synergy HT; BioTek Instruments, Winooski, VT). Composition fold change relative to day 0 was calculated as C_f/C_i (C_i: content immediately after cell loading; C_f: content after 7, 14, or 28 days of culture).

dsDNA—PicoGreen. Total dsDNA was quantified using a commercially available kit (Quant-iT PicoGreen dsDNA Assay Kit; Thermo Fisher Scientific). Fluorescence was measured at 480 and 520 nm and dsDNA quantified on a lambda DNA standard curve.

Total collagen—hydroxyproline. An equal volume of 6 N HCl was added to samples or serial dilutions of trans-4-hydroxy-L-proline (ACROS Organics™, Morris Plains, NJ) and incubated overnight at 110°C.[31] Samples were incubated for 5 min at room temperature following addition of 500 μL of oxidant solution (0.178 g Chloramines T in 15 mL of isopropanol and 10 mL of ddH_2O) and then 25 mL of acetate citrate buffer (120 g sodium acetate trihydrate, 12 mL acetic acid, 50 g citric acid monohydrate, and 34 g NaOH in 1 L ddH_2O, pH 6.0). Subsequently, 500 μL of Ehrlich's reagent (1 g p-dimethylaminobenzaldehyde (Sigma-Aldrich) in 20 mL isopropanol with 6.6 mL perchloric acid and 15.6 mL ddH_2O) was added and samples incubated at 60°C for 12 min. Following 4 min of cooling on ice, samples were transferred to a 96 well microtiter plate and absorbance read at 550 nm.

Sulfated glycosaminoglycan—dimethylmethylene blue. Sodium formate was added to 1, 9-dimethylmethylene blue (DMMB) in ethanol and the pH adjusted to 3.0 with formic acid to create the sGAG assay buffer.[32] Samples were combined with buffer in a microtiter plate and the sGAG concentration determined from absorbance at 520 nm and a chondroitin sulfate standard curve.

Total protein—Lowry assay. Samples were mixed with Biuret's reagent (Sigma-Aldrich) and maintained at room temperature for 12 min.[33] The absorbance at 650 nm was measured after 30 min at room temperature following addition of Folin–Ciocalteu's reagent (Sigma-Aldrich). Total

Table 1. Primer Sequences

Gene	*Forward primer (5′-3′)*	*Reverse primer (5′-3′)*	*Accession no.*
GAPDH	CGGGATTTGGTCGTATTG	CTGGAAGATGGTGATGGG	NM_001289746.1
ALPL	TTCTTCTTGCTGGTGGAG	GGCTTCTTGTCTGTGTCA	XM_017000903.1
COL1A1	AGAGCATGACCGATGGATTC	CCTTCTTGAGGTTGCCAGTC	XM_005257059.4
BGLAP	GCAGAGTCCAGCAAAGGT	CCCAGCCATTGATACAGG	NM_199173.5
CNR1	CGATACACTTGGCATTGACG	AACCACGAGCAAAGGAGAGA	XM_006715330.3
CNR2	ATTGGCAGCGTGACTATG	GAAGGCGATGAACAGGAG	XM_011540629.2
TNFRSF11B	AACCCCAGAGCGAAATAC	AAGAATGCCTCCTCACAC	NM_002546.3
TNFSF11	ATCGTTGGATCACAGCACATCA	TGAGCAAAAGGCTGAGCTTCA	XM_017020803.1

ALPL, alkaline phosphatase; *CNR1*, cannabinoid receptor type I; *CNR2*, cannabinoid receptor type II; *COL1A1*, collagen type 1α1; *GAPDH*, glyceraldehyde 3-phosphate dehydrogenase; *BGLAP*, osteocalcin; *TNFRSF11B*, osteoprotegerin; *TNFSF11*, receptor activator of nuclear factor kappa-β ligand.

protein concentration was determined on a bovine serum albumin (Sigma-Aldrich) standard curve.

Ultrastructure (days 0, 7, 14)

Individual samples were fixed in 0.5% glutaraldehyde in 0.1 M sodium cacodylate buffer (pH 7.4) for 1 h and then for 48 h in 0.1% osmium tetroxide. They were dehydrated in a series of ethanol solutions (50–100%), and, following critical point drying, sputter coated with gold. Photomicrographs were generated of SEM images (Quanta 200; FEI Company, Hillsboro, OR).

Statistical analyses

All results are presented as least squares mean ± SEM. Statistical analyses were performed with commercially available software (SAS 9.4; Institute, Cary, NC). A $3\times3\times3$ factorial analysis of variance followed by pairwise tests of least-squares means was used to compare gene expression and composition measures among time points, scaffolds, and media ($p<0.05$). Normality and homogeneity of variance were assessed with Shapiro–Wilk tests and residual plots.

Results

Cell viability (days 0, 7, 14)

Overall cell loading efficiency was 80.6% ± 3.4% and viability was similar among scaffolds immediately after loading (day 0, Fig. 1A). After 7 days of culture, the percentage of live cells was not significantly different among constructs irrespective of medium (Fig. 1B). After 14 days, the percentage of viable cells on CT constructs in S medium was significantly lower than C constructs (Fig. 1C).

Gene expression (days 7, 14, 28)

In general, *ALPL* expression tended to decrease and *BGLAP* increase with culture time, while *COL1A1* increased with culture S medium (Table 2 and Fig. 2). The changes in *ALPL* and *BGLAP* expression were most pronounced in HT scaffolds cultured in O medium. Summarily, there was highest expression of *ALPL* in HT constructs cultured in OS and O media after 7 days of culture. By 14 days of culture, *ALPL* expression was highest in HT and C constructs in O medium. After 28 days, the highest *ALPL* expression was in C constructs in O medium. The *COL1A1* expression was highest in C and HT constructs in O and OS media after 7 days and in S medium after 14 and 28 days of culture. By day 28, C and HT constructs cultured in O media had the highest *BGLAP* expression.

With time, *CNR1* and *TNFRSF11B/TNFSF11* expression tended to increase in constructs cultured in O medium (Table 2 and Fig. 3). The *CNR1* expression was highest in C constructs in O medium at all time points. Expression of *CNR2* was highest in C and CT constructs after 14 days of culture in all media. The *TNFRSF11B/TNFSF11* expression ratio was highest in on HT constructs in all media after 14 and 28 days, although the greatest expression was reached after 28 days in O medium.

Compositional analysis (days 7, 14, 28)

dsDNA—PicoGreen. The dsDNA fold change tended to remain the same or increase slightly with time (Table 3 and Fig. 4). It was highest on HT constructs in O medium after 7 days, in O and OS media after 14 days, and in S and OS media after 28 days of culture.

Total collagen—hydroxyproline. Total collagen fold change also increased slightly or remained static with time. Fold change was highest on C scaffolds for all time points and media.

Sulfated glycosaminoglycan—dimethylmethylene blue. The sGAG fold change tended to increase with time in C and HT constructs cultured in O and OS media. It was highest on HT constructs in OS and O medium after 7 days of culture and on C constructs after 28 days of culture in the same media.

Total protein—Lowry assay. Total protein fold change was primarily evident in C constructs, and it was highest on C constructs in S and O media after 14 days and in OS and O media after 28.

Scanning electron microscopy

Following cell loading, collagen fibrils tended to fuse with each other or other scaffold materials (Fig. 5). Amorphous matrix deposition was apparent in C constructs in S and O medium after 7 and 14 days of culture. In HT constructs, there was considerably more loosely organized, fibrous ECM following culture in S versus O medium and

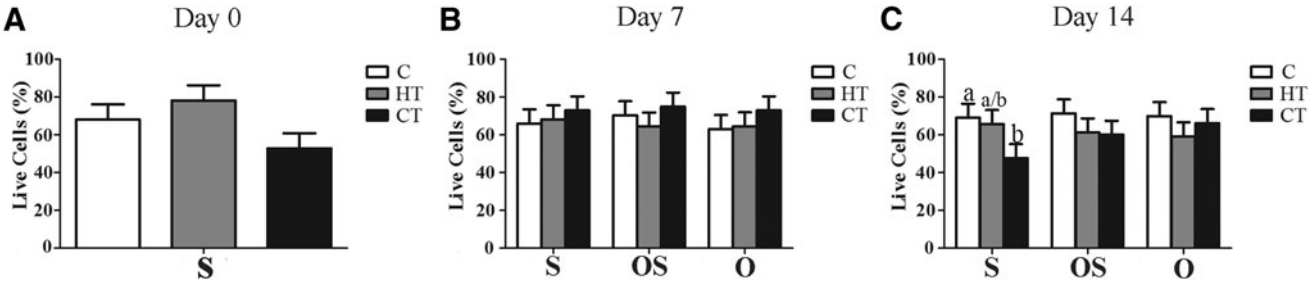

FIG. 1. Cell percentages (LS mean ± SEM) for type I bovine collagen (C), hydroxyapatite + β tricalcium phosphate + type I bovine collagen (HT), and β tricalcium phosphate + type I bovine (CT) scaffold-ASC constructs after 0 **(A)**, 7 **(B)**, and 14 **(C)** days of culture in stromal (S), osteogenic for 48 h followed by stromal (OS) or osteogenic (O) medium. Significant differences are indicated by *different column superscripts* within graphs ($p<0.05$). ASC, adipose-derived multipotent stromal cell; LS, least squares; SEM, standard error of the mean.

Table 2. Fold Change ($2^{-\Delta\Delta C_T}$) in *ALPL*, *COL1A1*, *BGLAP*, *CNR1*, *CNR2*, *TNFRSF11B/TNFSF11* (Mean ± SEM) Gene Expression in C, HT, and CT ASC-Scaffold Constructs Cultured in Stromal (S), Osteogenic for 48 h Followed by Stromal (OS) or Osteogenic (O) Medium for 7, 14, and 28 Days

		S			*OS*			*O*		
Gene	*Scaffold*	*Day 7*	*Day 14*	*Day 28*	*Day 7*	*Day 14*	*Day 28*	*Day 7*	*Day 14*	*Day 28*
ALPL	C	1.4 ± 1.7^{A}	6.7 ± 1.7^{B}	6.0 ± 1.7^{B}	3.0 ± 1.7^{A}	7.9 ± 1.7^{B}	9.9 ± 1.7^{B}	3.7 ± 1.7^{A}	18.1 ± 1.7^{B}	15.1 ± 1.7^{B}
	HT	3.4 ± 1.7^{A}	14.7 ± 1.7^{B}	10.2 ± 1.7^{B}	16.7 ± 1.7^{A}	11.4 ± 1.7^{B}	$12.7 \pm 1.7^{A/B}$	$11.8 \pm 1.7^{A/B}$	18.4 ± 1.7^{A}	9.1 ± 1.7^{B}
	CT	4.6 ± 1.7	4.0 ± 1.7	4.5 ± 1.7	3.2 ± 1.7	4.6 ± 1.7	2.2 ± 1.7	4.6 ± 1.7	5.1 ± 1.7	2.8 ± 1.7
COL1A1	C	1.0 ± 0.8^{A}	3.6 ± 0.8^{B}	4.0 ± 0.8^{B}	2.2 ± 0.8	1.2 ± 0.8	1.1 ± 0.8	2.2 ± 0.8	1.3 ± 0.8	0.6 ± 0.8
	HT	1.4 ± 0.8^{A}	5.3 ± 0.8^{B}	6.6 ± 0.8^{B}	2.0 ± 0.8	0.5 ± 0.8	0.5 ± 0.8	2.5 ± 0.8^{A}	$0.5 \pm 0.8^{A/B}$	0.2 ± 0.8^{B}
	CT	0.08 ± 0.8	0.9 ± 0.8	1.1 ± 0.8	0.8 ± 0.8	0.2 ± 0.8	0.4 ± 0.8	0.1 ± 0.8	0.2 ± 0.8	0.2 ± 0.8
BGLAP	C	1.1 ± 0.6^{A}	3.6 ± 0.6^{B}	5.1 ± 0.6^{C}	1.5 ± 0.6^{A}	4.1 ± 0.6^{B}	4.7 ± 0.6^{B}	1.9 ± 0.6^{A}	4.9 ± 0.6^{B}	6.8 ± 0.6^{B}
	HT	1.3 ± 0.6	1.9 ± 0.6	2.7 ± 0.6	1.1 ± 0.6	1.8 ± 0.6	2.2 ± 0.6	1.3 ± 0.6^{A}	2.3 ± 0.6^{A}	4.8 ± 0.6^{B}
	CT	0.9 ± 0.6	1.4 ± 0.6	1.9 ± 0.6	1.1 ± 0.6	1.9 ± 0.6	2.5 ± 0.6	0.9 ± 0.6	1.7 ± 0.6	2.3 ± 0.6
CNR1 ($\times 10^4$)	C	0.0006 ± 0.3	0.0003 ± 0.3	0.01 ± 0.3	0.002 ± 0.3	0.007 ± 0.3	0.03 ± 0.3	4 ± 0.3^{A}	4.6 ± 0.3^{B}	5.3 ± 0.3^{B}
	HT	0.0002 ± 0.3	0.0004 ± 0.3	0.03 ± 0.3	0.1 ± 0.3	0.03 ± 0.3	0.02 ± 0.3	0.3 ± 0.3^{A}	2.3 ± 0.3^{B}	1.1 ± 0.3^{C}
	CT	0.0001 ± 0.3	0.0002 ± 0.3	0.0003 ± 0.3	0.02 ± 0.3	0.01 ± 0.3	0.002 ± 0.3	0.02 ± 0.3^{A}	$0.6 \pm 0.3^{A/B}$	1.2 ± 0.3^{B}
CNR2	C	13.5 ± 4.8^{A}	39.9 ± 4.8^{B}	16.9 ± 4.8^{A}	8.1 ± 4.8	15.6 ± 4.8	12.8 ± 4.8	7.7 ± 4.8^{A}	40.3 ± 4.8^{B}	6.0 ± 4.8^{A}
	HT	3.0 ± 4.8	9.0 ± 4.8	5.1 ± 4.8	8.5 ± 4.8	7.8 ± 4.8	8.1 ± 4.8	9.3 ± 4.8	16.5 ± 4.8	18.1 ± 4.8
	CT	6.1 ± 4.8^{A}	36.1 ± 4.8^{B}	21.5 ± 4.8^{C}	6.6 ± 4.8^{A}	32.7 ± 4.8^{B}	16.9 ± 4.8^{A}	3.4 ± 4.8^{A}	22.2 ± 4.8^{B}	7.7 ± 4.8^{A}
TNFRSF11B/ TNFSF11	C	1.1 ± 2.5	2.6 ± 2.5	3.7 ± 2.5	2.1 ± 2.5	3.0 ± 2.5	7.8 ± 2.5	7.5 ± 2.5^{A}	6.2 ± 2.5^{A}	67.8 ± 2.5^{B}
	HT	4.1 ± 2.5^{A}	13.7 ± 2.5^{B}	15.7 ± 2.5^{B}	4.4 ± 2.5^{A}	16.1 ± 2.5^{B}	14.5 ± 2.5^{B}	2.7 ± 2.5^{A}	49.1 ± 2.5^{B}	90.4 ± 2.5^{C}
	CT	0.3 ± 2.5	0.8 ± 2.5	3.8 ± 2.5	0.2 ± 2.5	1.0 ± 2.5	2.4 ± 2.5	0.7 ± 2.5	3.9 ± 2.5	6.2 ± 2.5

Fold change was calculated relative to the reference gene *GAPDH* and target gene expression in constructs immediately after cell loading. Columns with different superscripts within constructs and media are significantly different among time points.

ASC, adipose-derived multipotent stromal cell; SEM, standard error of the mean.

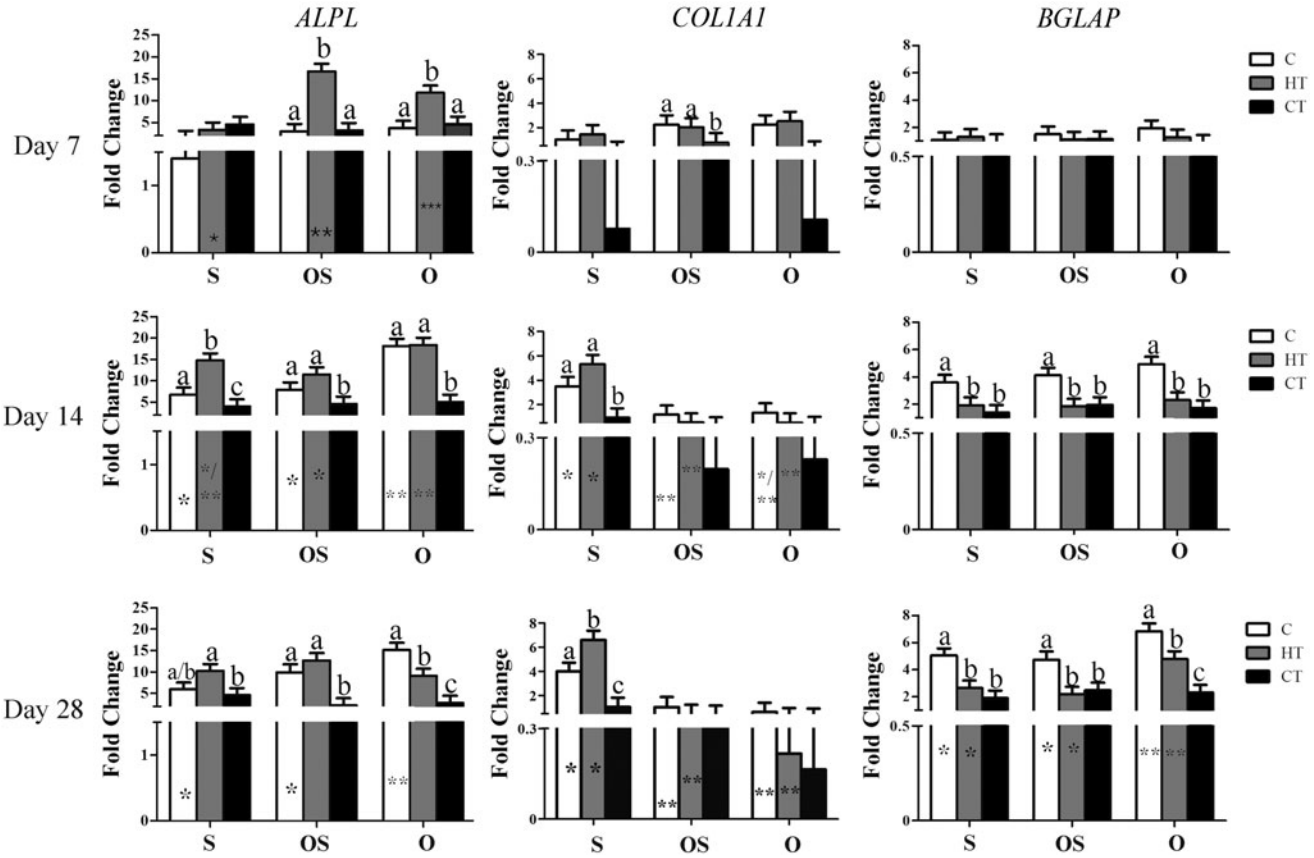

FIG. 2. Alkaline phosphatase (*ALPL*), collagen 1α1 (*COL1A1*) and osteocalcin (*BGLAP*) (LS mean ± SEM) expression in type I bovine collagen (C), hydroxyapatite + β tricalcium phosphate + type I bovine collagen (HT), and β tricalcium phosphate + type I bovine (CT) scaffold-ASC constructs cultured in stromal (S), osteogenic for 48 h followed by stromal (OS) or osteogenic (O) medium for 7, 14, or 28 days. The $2^{-\Delta\Delta Ct}$ values are reported relative to the reference gene glyceraldehyde 3-phosphate dehydrogenase (*GAPDH*) and target gene expression in constructs immediately after cell loading. Columns with distinct *superscripts* are significantly different among constructs within culture medium, and those with *different numbers* of *asterisks* (*) are significantly different among culture medium within constructs ($p < 0.05$).

the amount increased with culture time. Mineralized scaffold material was most prevalent in CT constructs. The ECM was more fibrous in CT constructs cultured in S versus O medium after 7 and 14 days of culture, but deposition was marginal compared with other constructs. Overall ECM deposition and organization was greatest in HT constructs cultured in O medium for 14 days.

Discussion

The results of this study indicate that HT and C scaffolds in O medium support more robust ASC osteogenesis than CT scaffolds. This was evidenced by early increases in *ALPL* expression, later increases in *BGLAP* expression, and ECM deposition and ultrastructure. Similar genetic expression and ECM deposition with higher collagen content on C scaffolds suggest comparable, although potentially slower osteogenesis and a strong propensity for a more fibrous matrix ultrastructure compared with HT scaffolds. A notable distinction between the cell–scaffold constructs was significantly higher *CNR1* expression on C scaffolds and *TNFRSF11B/TNFSF11* expression on HT scaffolds throughout the majority of the study. Together these results suggest that it is possible to customize ASC osteogenic cell signaling for enhanced bone formation based on bone pathology.

The time course of *ALPL* and *BGLAP* expression within HT constructs in O medium is consistent with osteoblastic differentiation and maturation.[34,35] HA in the HT scaffold may have been responsible for the initial enhanced *ALPL* expression over the other scaffolds since HA stimulates human ASC and BMSC *ALPL* expression[36,37] and ASC osteogenic differentiation.[38,39] The earliest increase in *ALPL* expression in this study was in O medium; however, the higher *ALPL* in HT constructs cultured in OS medium for 7 days and S medium for 14 days further supports the effect of the scaffold on the cells. Increased expression of *ALPL* and *BGLAP* in C constructs also suggests that collagen promotes osteoblastic ASC differentiation and maturation in O medium, although potentially not as robustly as HA.[40,41] This is further supported by lack of a decrease in *ALPL* expression in C constructs.[30] Genes for this study were selected to distinguish between early osteoblastic differentiation (*ALPL*), osteoblastic maturation (*BGLAP*), and osteoblastic activity (*COL1A1*) for comparisons among treatments.[42–44] The focus of this study was on early ASC direction and ECM production versus bone formation that is better described by later stage genes.[45]

Lower osteogenic gene expression and ECM deposition within CT constructs may be due tricalcium phosphate dissolution based on previous reports of lower proliferation

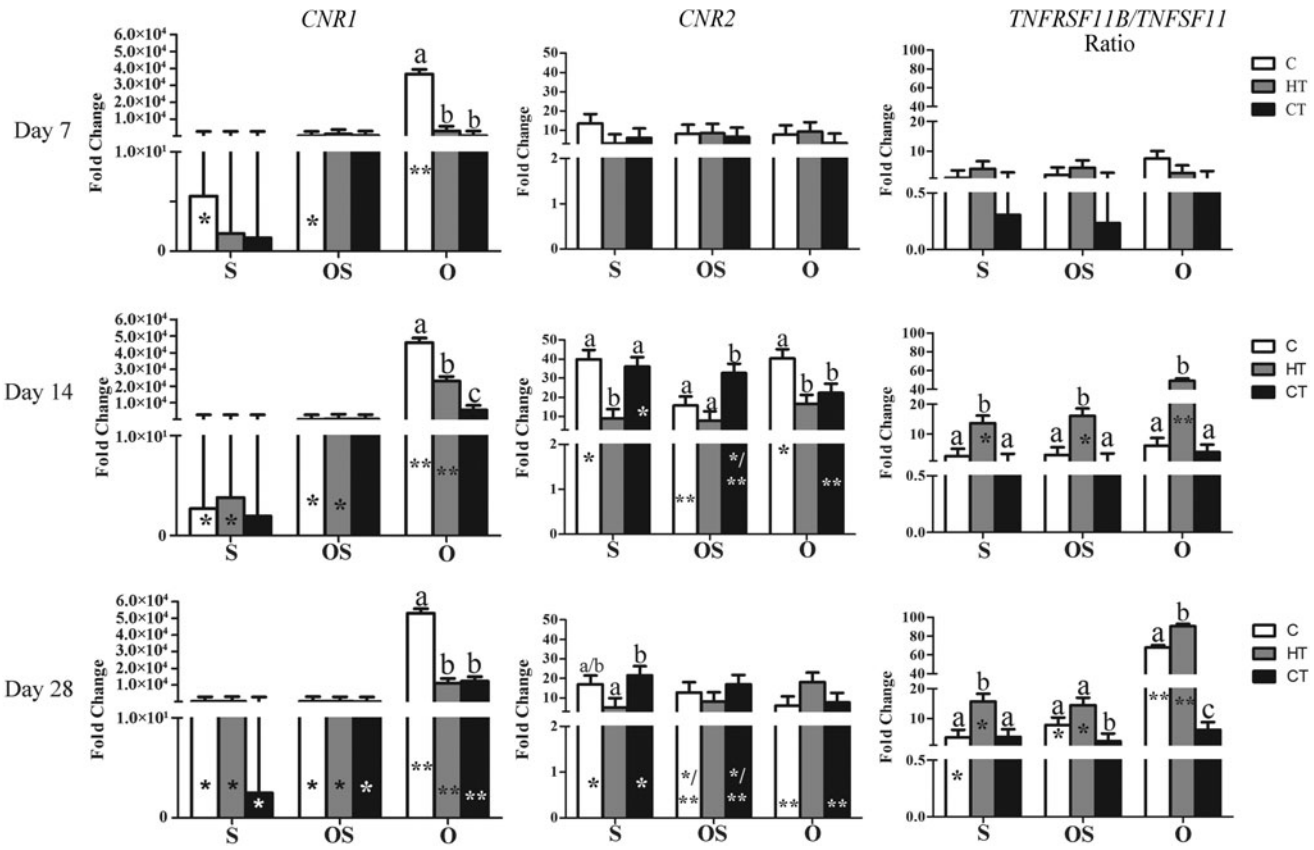

FIG. 3. Cannabinoid receptors type I (*CNR1*) and II (*CNR2*), and the ratio of osteoprotegerin and the receptor activator of nuclear factor kappa β ligand (*TNFRSF11B/TNFSF11*) (LS mean ± SEM) expression in the same scaffolds under identical culture conditions as Figure 2. Columns with distinct *superscripts* are significantly different among constructs within culture medium, and those with *different numbers* of *asterisks* (*) are significantly different among culture medium within constructs ($p < 0.05$).

and viability of undifferentiated cells on comparable scaffolds.[46] Since lower cell viability was only detected in S medium after 14 days, cell loss may not be the strongest contributor to the observed differences. Another possibility is that the high mineral content caused cell membrane damage or interfered with cell attachment required for differentiation, maturation, and ECM production.[47–49] Although surface roughness usually has a positive relationship with osteoblastic differentiation and matrix production, it can be inhibitory beyond a certain point.[50–52]

TABLE 3. FOLD CHANGE (MEAN ± SEM) IN DOUBLE-STRANDED DNA, TOTAL COLLAGEN, SGAG, AND PROTEIN IN C, HT, AND CT ASC-SCAFFOLD CONSTRUCTS CULTURED IN STROMAL (S), OSTEOGENIC FOR 48 H FOLLOWED BY STROMAL (OS) OR OSTEOGENIC (O) MEDIUM FOR 7, 14, AND 28 DAYS

		S			*OS*			*O*		
Component	*Scaffold*	*Day 7*	*Day 14*	*Day 28*	*Day 7*	*Day 14*	*Day 28*	*Day 7*	*Day 14*	*Day 28*
dsDNA	C	1.2 ± 0.2	1.1 ± 0.2	1.1 ± 0.2	1.1 ± 0.2	1.2 ± 0.2	1.1 ± 0.2	1.2 ± 0.2	1.3 ± 0.2	1.5 ± 0.2
	HT	1.6 ± 0.2^{A}	1.6 ± 0.2^{A}	2.6 ± 0.2^{B}	1.3 ± 0.2^{A}	2.6 ± 0.2^{B}	1.8 ± 0.2^{A}	2.5 ± 0.2^{A}	2.7 ± 0.2^{A}	1.8 ± 0.2^{B}
	CT	1.4 ± 0.2	1.5 ± 0.2	1.8 ± 0.2	1.5 ± 0.2	1.6 ± 0.2	1.4 ± 0.2	1.8 ± 0.2	1.8 ± 0.2	1.9 ± 0.2
Total collagen	C	1.5 ± 0.1^{A}	1.5 ± 0.1^{A}	2.2 ± 0.1^{B}	1.5 ± 0.1^{A}	2.0 ± 0.1^{B}	2.1 ± 0.1^{B}	2.2 ± 0.1	2.6 ± 0.1	2.2 ± 0.1
	HT	1.1 ± 0.1	1.0 ± 0.1	1.0 ± 0.1	1.4 ± 0.1	1.0 ± 0.1	1.2 ± 0.1	1.1 ± 0.1	1.0 ± 0.1	1.1 ± 0.1
	CT	1.1 ± 0.1	0.9 ± 0.1	0.9 ± 0.1	0.9 ± 0.1	0.9 ± 0.1	0.9 ± 0.1	1.0 ± 0.1	1.0 ± 0.1	0.9 ± 0.1
sGAG	C	1.1 ± 0.2	1.7 ± 0.2	1.7 ± 0.2	1.2 ± 0.2^{A}	1.8 ± 0.2^{A}	3.3 ± 0.2^{B}	1.3 ± 0.2^{A}	2.6 ± 0.2^{B}	2.8 ± 0.2^{B}
	HT	1.2 ± 0.2	1.6 ± 0.2	1.6 ± 0.2	2.1 ± 0.2^{A}	1.2 ± 0.2^{B}	2.1 ± 0.2^{A}	2.5 ± 0.2	2.5 ± 0.2	2.1 ± 0.2
	CT	1.1 ± 0.2	1.4 ± 0.2	1.6 ± 0.2	1.3 ± 0.2	1.4 ± 0.2	1.1 ± 0.2	1.6 ± 0.2	1.8 ± 0.2	1.6 ± 0.2
Protein	C	1.0 ± 0.1	1.3 ± 0.1	1.1 ± 0.1	1.1 ± 0.1	1.1 ± 0.1	1.5 ± 0.1	1.2 ± 0.1	1.7 ± 0.1	1.4 ± 0.1
	HT	1.0 ± 0.1	1.1 ± 0.1	1.0 ± 0.1	1.1 ± 0.1	1.0 ± 0.1	1.1 ± 0.1	1.1 ± 0.1	1.0 ± 0.1	1.1 ± 0.1
	CT	1.0 ± 0.1	1.0 ± 0.1	1.0 ± 0.1	1.0 ± 0.1	0.9 ± 0.1	1.0 ± 0.1	1.1 ± 0.1	1.0 ± 0.1	1.1 ± 0.1

Individual values (unitless) were calculated relative to day 0 as C_f/C_i where C_i is content immediately after cell loading and C_f is content after 7, 14, or 28 days of culture. Columns with different superscripts within constructs and media are significantly different among test time points.

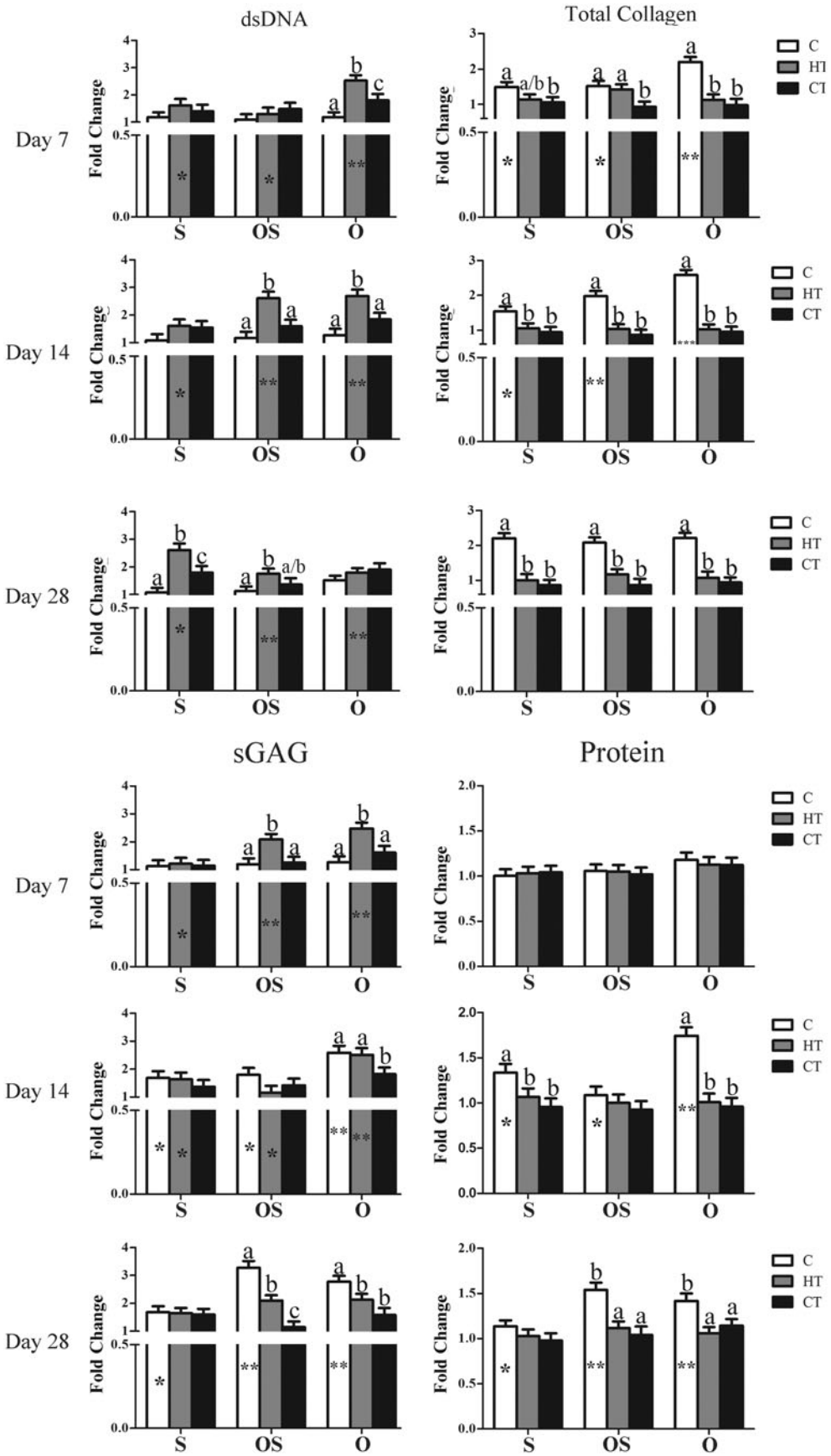

FIG. 4. Fold change in dsDNA, total collagen, sulfated glycosaminoglycan (sGAG) and protein content (LS mean ± SEM) in the same constructs and media as Figure 2 after 7, 14, or 28 days of culture. Columns with distinct *superscripts* are significantly different among constructs within culture medium and those with *different numbers* of *asterisks* (*) are significantly different among culture medium within constructs ($p < 0.05$).

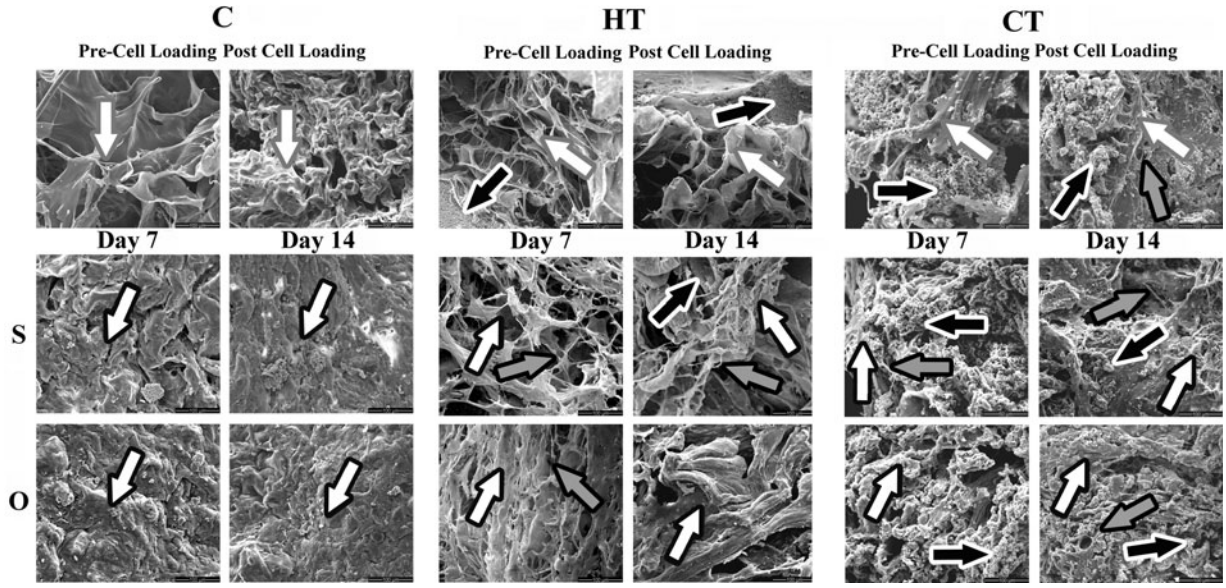

FIG. 5. Scanning electron photomicrographs of human ASC-scaffold constructs composed of bovine collagen type I (C), hydroxyapatite + β-tricalcium phosphate + bovine collagen type I (HT) and β tricalcium phosphate + bovine collagen type 1 (CT) before (Pre-Cell Loading) and after (Post Cell Loading) spinner flask cell loading and after 7 (Day 7) and 14 (Day 14) days of culture in stromal (S) or osteogenic (O) medium. Black arrows with white outline: mineralized scaffold; grey arrows with black outline: collagen fibrils; white arrows with black outline: extra-cellular matrix; white arrows with grey outline: scaffold.

Genetic expression is a standard mechanism to evaluate and compare cell characteristics that are important to quantify changes induced by medium or scaffold as in this study.[53] Genetic expression does not entirely reflect cell function in terms of matrix production,[54] a central point of directed osteogenesis.[49] ECM production is central to the self-perpetuating cycle of ossification.[55] Determination of differences in ECM content provides a mechanism to assess and quantify the process and provide a more comprehensive evaluation of treatment effects on cell behaviors than genetic analysis alone.[56,57] Generally, increases in dsDNA suggest cell proliferation associated with lack of differentiation.[49] Proteoglycan, collagen, and protein synthesis occurs throughout ossification primarily from osteoblastic ECM production.[55] As such, the ECM content and ultrastructure help to confirm tissue changes suggested by gene expression.

While there was some evidence of osteogenic stimulation from culture in OS medium, it did not support the same level as continuous O medium culture. The short-term exposure in this study may not have been sufficient to induce osteoblastic differentiation in the entire cell population within the scaffolds since isolates may have contained cells at various stages of differentiation.[27] Nonetheless, there was a genetic effect of short-term osteogenic medium exposure as indicated by higher *ALPL* expression at day 7 on HT scaffolds cultured in OS versus S medium. Similarly, lower *COL1A1* expression on C and HT scaffolds in the OS group that mirrored that of scaffolds cultured in O medium after 14 and 28 days of culture suggest cell maturation. Further support of the impact of OS medium included increased ECM protein, sGAG, collagen, and dsDNA over S medium at various points in the study. The variable increases in osteogenic gene expression and ECM components are consistent with a cell population with variable maturity.[58] Nonetheless, the observed genetic upregulation and increased ECM components confirm that there is some benefit to short-term exposure of ASC-scaffold constructs to osteogenic medium.[57] Customization of medium and culture period will likely increase the effects.

Collagen upregulation and ECM deposition in C constructs in all culture media observed in this study may be a result of collagen type I stimulation of extracellular signal-regulated protein kinase (ERK).[59] Coating cultureware with collagen increases ERK phosphorylation and expression of *ALPL* and *BGLAP* in human ASCs.[60] The results of this study are consistent with these earlier findings and may indicate that high collagen content scaffolds promote ASC osteoblastic differentiation and ECM production, but slightly less than scaffolds with both collagen and a mixture of inorganic minerals. The importance of this difference in patients with compromised bone formation may not be relevant long term, so upregulation of the specific signaling pathways discussed below may be the strongest mechanism for therapeutic improvements.

Scaffold effects on *CNR1* and the *TNFRSF11B/TNFSF11* ratio expression were the notable distinction among C and HT constructs cultured in O medium. The importance of *CNR1* for MSC osteogenic differentiation has been established. It increases with MSC osteoblastic differentiation,[10,61] and BMSCs from *CNR1* knockouts have a reduced capacity for osteoblastic differentiation.[9] The role of *CNR1* in bone homeostasis appears to be mediated primarily through adrenergic signaling and separate from the Wnt signaling pathway.[13,62] Of importance to clinical translation is that lower *CNR1* expression is associated with age-related bone loss and increased marrow adiposity.[9,10]

The ratio of *TNFRSF11B/TNFSF11* drives osteoblastic differentiation through increases in *TNFRSF11B* or decreases in *TNFSF11* and *TNFRSF11B* expression is mediated through Wnt/β-catenin pathways.[63–68] Disruption of the

TNFRSF11B/TNFSF11 ratio is more closely aligned with bone pathology versus bone aging associated with changes in *CNR1* expression.[69,70] In contrast to the *CNR1* signaling pathway apparent in C constructs discussed above, an increase in *TNFRSF11B/TNFSF11* expression was consistently apparent in HT constructs. The source of the difference may be that HA increases low-density lipoprotein receptor-related protein 5 and β-catenin expression, and both stimulate canonical Wnt.[64–66,71]

Increased *CNR2* expression after 14 days of culture in all media and constructs suggests less association with ASC osteogenesis than other genes. The role of *CNR2* in the regulation of bone metabolism is not well defined, and existing information suggests both a supportive and an inhibitory effect of *CNR2* on MSC osteogenesis.[10,12,72,73]

These results support the capability of human ASCs to be directed toward different osteogenic pathways by scaffold substrate characteristics. This information may help guide targeted research for distinct bone pathology. Local therapy based on predominant needs of the recipient may be a safe and effective alternative to systemic activation of both cannabinoid and Wnt signaling, which are both associated with serious side effects.[11,68,74–76] The complexity of and overlap between signaling pathways, however, requires further work to confirm distinct pathways at multiple levels between treatments.[63]

The parallel outcome measures in this study indicate that HT scaffolds in osteogenic medium have the highest *in vitro* ASC osteogenesis followed closely by C. Further, osteogenesis appears to be mediated through distinct cell signaling pathways by C and HT scaffolds. This may indicate a significant value of considering patient characteristics when selecting bone grafts, especially when combining them with exogenous ASCs. Since underlying bone pathology may limit *in vivo* response to scaffolds with or without exogenous cells, the findings must be confirmed *in vivo* before general application. Nonetheless, it is possible that native osteogenesis may benefit more from some bone graft materials augmented by ASCs than others. Furthermore, this information creates a foundation for criteria to create autologous, viable bone grafts from adult ASCs to locally treat deficient bone-forming capacity.

Acknowledgments

This work was funded, in part, by the Louisiana Board of Regents Pilot Funding for New Research as well as the Louisiana State University School of Veterinary Medicine Competitive Organized Research Program. The authors thank Dr. Jeffrey Gimble for donating the human ASCs.

Disclosure Statement

No competing financial interests exist.

References

1. García-Gareta, E., Coathup, M.J., and Blunn, G.W. Osteoinduction of bone grafting materials for bone repair and regeneration. Bone **81,** 112, 2015.
2. Delloye, C., Cornu, O., Druez, V., and Barbier, O. Bone allografts. Bone Joint J **89,** 574, 2007.
3. Laurencin, C., Khan, Y., and El-Amin, S.F. Bone graft substitutes. Expert Rev Med Devices **3,** 49, 2014.
4. Bosetti, M., Bianchi, A.E., Zaffe, D., and Cannas, M. Comparative in vitro study of four commercial biomaterials used for bone grafting. J Appl Biomater Funct Mater **11,** e80, 2013.
5. Grottkau, B.E., and Lin, Y. Osteogenesis of adipose-derived stem cells. Bone Res **1,** 133, 2013.
6. Bergman, R., Gazit, D., Kahn, A., Gruber, H., McDougall, S., and Hahn, T. Age-related changes in osteogenic stem cells in mice. J Bone Miner Res **11,** 568, 1996.
7. Uccelli, A., Moretta, L., and Pistoia, V. Mesenchymal stem cells in health and disease. Nat Rev Immunol **8,** 726, 2008.
8. Silva, I., and Branco, J. Rank/Rankl/opg: literature review. Acta Reumatol Port **36,** 2011.
9. Idris, A.I., Sophocleous, A., Landao-Bassonga, E., Canals, M., Milligan, G., Baker, D., van't Hof, R.J., and Ralston, S.H. Cannabinoid receptor type 1 protects against age-related osteoporosis by regulating osteoblast and adipocyte differentiation in marrow stromal cells. Cell Metab **10,** 139, 2009.
10. Galve-Roperh, I., Chiurchiù, V., Díaz-Alonso, J., Bari, M., Guzmán, M., and Maccarrone, M. Cannabinoid receptor signaling in progenitor/stem cell proliferation and differentiation. Prog Lipid Res **52,** 633, 2013.
11. Idris, A.I., van't Hof, R.J., Greig, I.R., Ridge, S.A., Baker, D., Ross, R.A., and Ralston, S.H. Regulation of bone mass, bone loss and osteoclast activity by cannabinoid receptors. Nat Med **11,** 774, 2005.
12. Ofek, O., Karsak, M., Leclerc, N., Fogel, M., Frenkel, B., Wright, K., Tam, J., Attar-Namdar, M., Kram, V., and Shohami, E. Peripheral cannabinoid receptor, CB2, regulates bone mass. Proc Natl Acad Sci U S A **103,** 696, 2006.
13. Tam, J., Trembovler, V., Di Marzo, V., Petrosino, S., Leo, G., Alexandrovich, A., Regev, E., Casap, N., Shteyer, A., and Ledent, C. The cannabinoid CB1 receptor regulates bone formation by modulating adrenergic signaling. FASEB J **22,** 285, 2008.
14. Kondo, H., Takeuchi, S., and Togari, A. β-Adrenergic signaling stimulates osteoclastogenesis via reactive oxygen species. Am J Physiol Endocrinol Metab **304,** E507, 2013.
15. Ferreira, A.M., Gentile, P., Chiono, V., and Ciardelli, G. Collagen for bone tissue regeneration. Acta Biomater **8,** 3191, 2012.
16. Lee, C.H., Singla, A., and Lee, Y. Biomedical applications of collagen. Int J Pharm **221,** 1, 2001.
17. Van Hoff, C., Samora, J., Griesser, M.J., Crist, M.K., Scharschmidt, T., and Mayerson, J.L. Effectiveness of ultraporous β-tricalcium phosphate (vitoss) as bone graft substitute for cavitary defects in benign and low-grade malignant bone tumors. Am J Orthop (Belle Mead, NJ) **41,** 20, 2012.
18. Wu, S., Liu, X., Yeung, K.W., Liu, C., and Yang, X. Biomimetic porous scaffolds for bone tissue engineering. Mater Sci Eng R Rep **80,** 1, 2014.
19. Chan, B.P., Hui, T.Y., Wong, M.Y., Yip, K.H.K., and Chan, G.C.F. Mesenchymal stem cell-encapsulated collagen microspheres for bone tissue engineering. Tissue Eng Part C Methods **16,** 225, 2009.
20. Inzana, J.A., Olvera, D., Fuller, S.M., Kelly, J.P., Graeve, O.A., Schwarz, E.M., Kates, S.L., and Awad, H.A. 3D printing of composite calcium phosphate and collagen scaffolds for bone regeneration. Biomaterials **35,** 4026, 2014.

21. Miguel, F.B., Júnior, A.d.A.B., de Paula, F.L., Barreto, I.C., Goissis, G., and Rosa, F.P. Regeneration of critical bone defects with anionic collagen matrix as scaffolds. J Mater Sci Mater Med **24,** 2567, 2013.
22. Damron, T.A. Use of 3D β-tricalcium phosphate (Vitoss®) scaffolds in repairing bone defects. Nanomedicine (Lond) **2,** 763, 2007.
23. Dawson, E., Bae, H.W., Burkus, J.K., Stambough, J.L., and Glassman, S.D. Recombinant human bone morphogenetic protein-2 on an absorbable collagen sponge with an osteoconductive bulking agent in posterolateral arthrodesis with instrumentation. J Bone Joint Surg **91,** 1604, 2009.
24. Meinel, L., Karageorgiou, V., Fajardo, R., Snyder, B., Shinde-Patil, V., Zichner, L., Kaplan, D., Langer, R., and Vunjak-Novakovic, G. Bone tissue engineering using human mesenchymal stem cells: effects of scaffold material and medium flow. Ann Biomed Eng **32,** 112, 2004.
25. You, M.-H., Kwak, M.K., Kim, D.-H., Kim, K., Levchenko, A., Kim, D.-Y., and Suh, K.-Y. Synergistically enhanced osteogenic differentiation of human mesenchymal stem cells by culture on nanostructured surfaces with induction media. Biomacromolecules **11,** 1856, 2010.
26. Polini, A., Pisignano, D., Parodi, M., Quarto, R., and Scaglione, S. Osteoinduction of human mesenchymal stem cells by bioactive composite scaffolds without supplemental osteogenic growth factors. PLoS One **6,** e26211, 2011.
27. Castano-Izquierdo, H., Álvarez-Barreto, J., Dolder, J.v.d., Jansen, J.A., Mikos, A.G., and Sikavitsas, V.I. Pre-culture period of mesenchymal stem cells in osteogenic media influences their in vivo bone forming potential. J Biomed Mater Res Part A **82A,** 129, 2007.
28. Thirumala, S., Gimble, J.M., and Devireddy, R.V. Evaluation of methylcellulose and dimethyl sulfoxide as the cryoprotectants in a serum-free freezing media for cryopreservation of adipose-derived adult stem cells. Stem Cells Dev **19,** 513, 2010.
29. Zhang, N., Dietrich, M.A., and Lopez, M.J. Canine intra-articular multipotent stromal cells (MSC) from adipose tissue have the highest in vitro expansion rates, multipotentiality, and MSC immunophenotypes. Vet Surg **42,** 137, 2013.
30. Xie, L., Zhang, N., Marsano, A., Vunjak-Novakovic, G., Zhang, Y., and Lopez, M.J. In vitro mesenchymal trilineage differentiation and extracellular matrix production by adipose and bone marrow derived adult equine multipotent stromal cells on a collagen scaffold. Stem Cell Rev Rep **9,** 858, 2013.
31. Edwards, C., and O'brien, W. Modified assay for determination of hydroxyproline in a tissue hydrolyzate. Clin Chim Acta **104,** 161, 1980.
32. Enobakhare, B.O., Bader, D.L., and Lee, D.A. Quantification of sulfated glycosaminoglycans in chondrocyte/alginate cultures, by use of 1, 9-dimethylmethylene blue. Anal Biochem **243,** 189, 1996.
33. Ohnishi, S.T., and Barr, J.K. A simplified method of quantitating protein using the biuret and phenol reagents. Anal Biochem **86,** 193, 1978.
34. Ilmer, M., Karow, M., Geissler, C., Jochum, M., and Neth, P. Human osteoblast-derived factors induce early osteogenic markers in human mesenchymal stem cells. Tissue Eng A **15,** 2397, 2009.
35. Nakamura, A., Dohi, Y., Akahane, M., Ohgushi, H., Nakajima, H., Funaoka, H., and Takakura, Y. Osteocalcin secretion as an early marker of in vitro osteogenic differentiation of rat mesenchymal stem cells. Tissue Eng C Methods **15,** 169, 2009.
36. Matsushima, A., Kotobuki, N., Tadokoro, M., Kawate, K., Yajima, H., Takakura, Y., and Ohgushi, H. In vivo osteogenic capability of human mesenchymal cells cultured on hydroxyapatite and on β-tricalcium phosphate. Artif Organs **33,** 474, 2009.
37. Osathanon, T., Chuenjitkuntaworn, B., Nowwarote, N., Supaphol, P., Sastravaha, P., Subbalekha, K., and Pavasant, P. The responses of human adipose-derived mesenchymal stem cells on polycaprolactone-based scaffolds: an in vitro study. Tissue Eng Regen Med **11,** 239, 2014.
38. Zuk, P.A. Tissue engineering craniofacial defects with adult stem cells? Are we ready yet? Pediatr Res **63,** 478, 2008.
39. Zanetti, A.S., Sabliov, C., Gimble, J.M., and Hayes, D.J. Human adipose-derived stem cells and three-dimensional scaffold constructs: a review of the biomaterials and models currently used for bone regeneration. J Biomed Mater Res B Appl Biomater **101,** 187, 2013.
40. Ngiam, M., Liao, S., Patil, A.J., Cheng, Z., Chan, C.K., and Ramakrishna, S. The fabrication of nano-hydroxyapatite on PLGA and PLGA/collagen nanofibrous composite scaffolds and their effects in osteoblastic behavior for bone tissue engineering. Bone **45,** 4, 2009.
41. Teng, S.-H., Lee, E.-J., Park, C.-S., Choi, W.-Y., Shin, D.-S., and Kim, H.-E. Bioactive nanocomposite coatings of collagen/hydroxyapatite on titanium substrates. J Mater Sci Mater Med **19,** 2453, 2008.
42. Stein, G.S., and Lian, J.B. Molecular mechanisms mediating proliferation/differentiation interrelationships during progressive development of the osteoblast phenotype. Endocr Rev **14,** 424, 1993.
43. Valenti, M.T., Dalle Carbonare, L., Donatelli, L., Bertoldo, F., Zanatta, M., and Cascio, V.L. Gene expression analysis in osteoblastic differentiation from peripheral blood mesenchymal stem cells. Bone **43,** 1084, 2008.
44. Aubin, J., Liu, F., Malaval, L., and Gupta, A. Osteoblast and chondroblast differentiation. Bone **17,** S77, 1995.
45. Qi, H., Aguiar, D.J., Williams, S.M., La Pean, A., Pan, W., and Verfaillie, C.M. Identification of genes responsible for osteoblast differentiation from human mesodermal progenitor cells. Proc Natl Acad Sci **100,** 3305, 2003.
46. Liu, Q., Cen, L., Yin, S., Chen, L., Liu, G., Chang, J., and Cui, L. A comparative study of proliferation and osteogenic differentiation of adipose-derived stem cells on akermanite and β-TCP ceramics. Biomaterials **29,** 4792, 2008.
47. Liu, Y., Cooper, P.R., Barralet, J.E., and Shelton, R.M. Influence of calcium phosphate crystal assemblies on the proliferation and osteogenic gene expression of rat bone marrow stromal cells. Biomaterials **28,** 1393, 2007.
48. Meredith, J., Fazeli, B., and Schwartz, M. The extracellular matrix as a cell survival factor. Mol Biol Cell **4,** 953, 1993.
49. Datta, N., Holtorf, H.L., Sikavitsas, V.I., Jansen, J.A., and Mikos, A.G. Effect of bone extracellular matrix synthesized in vitro on the osteoblastic differentiation of marrow stromal cells. Biomaterials **26,** 971, 2005.
50. Zan, X., Sitasuwan, P., Feng, S., and Wang, Q. Effect of roughness on in situ biomineralized CaP-collagen coating on the osteogenesis of mesenchymal stem cells. Langmuir **32,** 1808, 2016.
51. Deligianni, D.D., Katsala, N.D., Koutsoukos, P.G., and Missirlis, Y.F. Effect of surface roughness of hydroxyap-

atite on human bone marrow cell adhesion, proliferation, differentiation and detachment strength. Biomaterials **22,** 87, 2000.
52. Faia-Torres, A.B., Guimond-Lischer, S., Rottmar, M., Charnley, M., Goren, T., Maniura-Weber, K., Spencer, N.D., Reis, R.L., Textor, M., and Neves, N.M. Differential regulation of osteogenic differentiation of stem cells on surface roughness gradients. Biomaterials **35,** 9023, 2014.
53. Stevens, M.M. Biomaterials for bone tissue engineering. Mater Today **11,** 18, 2008.
54. Cote, A.J., McLeod, C.M., Farrell, M.J., McClanahan, P.D., Dunagin, M.C., Raj, A., and Mauck, R.L. Single-cell differences in matrix gene expression do not predict matrix deposition. Nat Commun **7,** 10865, 2016.
55. Ortega, N., Behonick, D.J., and Werb, Z. Matrix remodeling during endochondral ossification. Trends Cell Biol **14,** 86, 2004.
56. Eyre, D.R., and Weis, M.A. Bone collagen: new clues to its mineralization mechanism from recessive osteogenesis imperfecta. Calcif Tissue Int **93,** 338, 2013.
57. Salbach-Hirsch, J., Ziegler, N., Thiele, S., Moeller, S., Schnabelrauch, M., Hintze, V., Scharnweber, D., Rauner, M., and Hofbauer, L.C. Sulfated glycosaminoglycans support osteoblast functions and concurrently suppress osteoclasts. J Cell Biochem **115,** 1101, 2014.
58. Lin, Z., Rios, H.F., Volk, S.L., Sugai, J.V., Jin, Q., and Giannobile, W.V. Gene expression dynamics during bone healing and osseointegration. J Periodontol **82,** 1007, 2011.
59. Kundu, A.K., and Putnam, A.J. Vitronectin and collagen I differentially regulate osteogenesis in mesenchymal stem cells. Biochem Biophys Res Commun **347,** 347, 2006.
60. Salasznyk, R.M., Klees, R.F., Hughlock, M.K., and Plopper, G.E. ERK signaling pathways regulate the osteogenic differentiation of human mesenchymal stem cells on collagen I and vitronectin. Cell Commun Adhes **11,** 137, 2004.
61. Gowran, A., McKayed, K., and Campbell, V.A. The cannabinoid receptor type 1 is essential for mesenchymal stem cell survival and differentiation: implications for bone health. Stem Cells Int **2013,** 796715, 2013.
62. Hendaoui, I., Lavergne, E., Lee, H.-S., Hong, S.H., Kim, H.-Z., Parent, C., Heuzé-Vourc'h, N., Clément, B., and Musso, O. Inhibition of Wnt/β-catenin signaling by a soluble collagen-derived frizzled domain interacting with Wnt3a and the receptors frizzled 1 and 8. PLoS One **7,** e30601, 2012.
63. Boyce, B.F., and Xing, L. Functions of RANKL/RANK/OPG in bone modeling and remodeling. Arch Biochem Biophys **473,** 139, 2008.
64. Kim, K., Dean, D., Lu, A., Mikos, A.G., and Fisher, J.P. Early osteogenic signal expression of rat bone marrow stromal cells is influenced by both hydroxyapatite nanoparticle content and initial cell seeding density in biodegradable nanocomposite scaffolds. Acta Biomater **7,** 1249, 2011.
65. Wu, X., Walker, J., Zhang, J., Ding, S., and Schultz, P.G. Purmorphamine induces osteogenesis by activation of the hedgehog signaling pathway. Chem Biol **11,** 1229, 2004.
66. Mao, L., Liu, J., Zhao, J., Chang, J., Xia, L., Jiang, L., Wang, X., Lin, K., and Fang, B. Effect of micro-nano-hybrid structured hydroxyapatite bioceramics on osteogenic and cementogenic differentiation of human periodontal ligament stem cell via Wnt signaling pathway. Int J Nanomed **10,** 7031, 2015.
67. Thorfve, A., Lindahl, C., Xia, W., Igawa, K., Lindahl, A., Thomsen, P., Palmquist, A., and Tengvall, P. Hydroxyapatite coating affects the Wnt signaling pathway during peri-implant healing in vivo. Acta Biomater **10,** 1451, 2014.
68. Krishnan, V., Bryant, H.U., and MacDougald, O.A. Regulation of bone mass by Wnt signaling. J Clin Invest **116,** 1202, 2006.
69. Blair, J.M., Zhou, H., Seibel, M.J., and Dunstan, C.R. Mechanisms of disease: roles of OPG, RANKL and RANK in the pathophysiology of skeletal metastasis. Nat Clin Pract Oncol **3,** 41, 2006.
70. Hofbauer, L., Kuhne, C., and Viereck, V. The OPG/RANKL/RANK system in metabolic bone diseases. J Musculoskelet Neuronal Interact **4,** 268, 2004.
71. Liu, D.D., Zhang, J.C., Zhang, Q., Wang, S.X., and Yang, M.S. TGF-β/BMP signaling pathway is involved in cerium-promoted osteogenic differentiation of mesenchymal stem cells. J Cell Biochem **114,** 1105, 2013.
72. Palazuelos, J., Davoust, N., Julien, B., Hatterer, E., Aguado, T., Mechoulam, R., Benito, C., Romero, J., Silva, A., and Guzmán, M. The CB2 cannabinoid receptor controls myeloid progenitor trafficking involvement in the pathogenesis of an animal model of multiple sclerosis. J Biol Chem **283,** 13320, 2008.
73. Ofek, O., Attar-Namdar, M., Kram, V., Dvir-Ginzberg, M., Mechoulam, R., Zimmer, A., Frenkel, B., Shohami, E., and Bab, I. CB2 cannabinoid receptor targets mitogenic Gi protein–cyclin D1 axis in osteoblasts. J Bone Miner Res **26,** 308, 2011.
74. Makowiecka, J., and Wielgus, K. Therapeutic potential of cannabinoids—perspectives for the future. J Nat Fibers **11,** 283, 2014.
75. Gregory, C.A., Gunn, W.G., Reyes, E., Smolarz, A.J., Munoz, J., Spees, J.L., and Prockop, D.J. How Wnt signaling affects bone repair by mesenchymal stem cells from the bone marrow. Ann N Y Acad Sci **1049,** 97, 2005.
76. Wada, T., Nakashima, T., Hiroshi, N., and Penninger, J.M. RANKL-RANK signaling in osteoclastogenesis and bone disease. Trends Mol Med **12,** 17, 2006.

Address correspondence to:
Mandi Lopez, DVM, MS, PhD
Department of Veterinary Clinical Sciences
Louisiana State University
School of Veterinary Medicine
1909 Skip Bertman Drive
Baton Rouge, LA 70803

E-mail: mlopez@lsu.edu

Received: February 16, 2017
Accepted: July 19, 2017
Online Publication Date: October 6, 2017